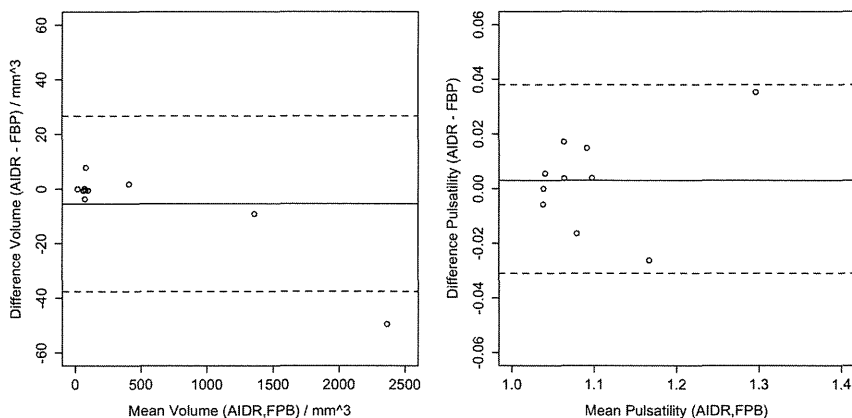**FIG 2.** Edge lengths compared between AIDR and FBP and edge length compared with intra-aneurysmal attenuation (*triangles*, left side; *dots*, right side). On the left side, a Bland-Altman plot shows a small bias of shorter edges in AIDR images. Th right side shows the plot and regression line of edge length and intra-aneurysmal attenuation ($P = .45$).

FIG 3. Bland-Altman plots of absolute volumes and pulsatility. Left side shows a small bias, with a tendency toward smaller absolute volumes in AIDR images. On the right side, there are no differences in pulsatility between the aneurysms in AIDR and FBP images.
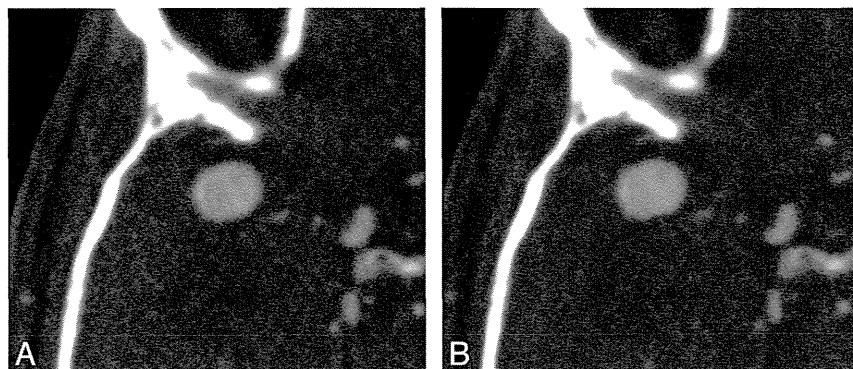
FIG 4. Aneurysm of the right middle cerebral artery in a 53-year-old patient (patient 1). CT angiography of the 2 reconstruction methods; acquisition parameters are the same. *A*, Filtered back-projection. *B*, Image reconstruction with adaptive iterative dose reduction. Note the smoother appearance of the image, consistent with reduced image noise.

time point zero. This initial cutting line was transferred automatically to all other time points by using an iterative closest-point approach, to reduce interaction time. Now, the surface model of the aneurysm for each time point was generated on the basis of the transferred cutting lines. For analysis, the absolute volumes and maximum and minimum volumes of the aneurysm surface model within the cardiac cycle were calculated and compared between both groups. Pulsatility was calculated as the ratio of maximum and minimum volumes and was compared between both groups.

RESULTS

Noise
In ROIs placed in the air, mean intensity values were -1040.2 ± 22.2 HU versus -1040.6 ± 22.1 HU ($P = .97$) and SDs were 9.8 ± 4.0 HU versus 8.0 ± 2.5 HU ($P = .04$) (FBP versus AIDR). In brain parenchyma, the means were 53.7 ± 5.0 HU versus 53.9 ± 4.8 HU ($P = .91$) and the SDs were 15.0 ± 3.5 HU versus 11.9 ± 1.9 HU ($P = .03$) (FBP versus AIDR); and in aneurysms, the means were 433.0 ± 136.1 HU versus 427.0 ± 132.6 HU ($P = .89$) and the SDs were 20.3 ± 7.4 HU versus 14.6 ± 5.2 HU ($P < .001$) (FBP versus AIDR).

Edge Sharpness
Mean edge length was 3.50 ± 0.49 mm versus 3.42 ± 0.49 mm (FBP versus AIDR). Bland-Altmann analysis revealed a bias of -0.08 mm (AIDR-FBP, $P = .06$, paired t test) and limits of agreement between -0.32 and 0.19 mm. Edge sharpness did not correlate significantly with intraluminal attenuation ($P = .45$, $r^2 = 0.032$) (Fig 2).

Absolute Volumes
Mean aneurysm size was 461.7 ± 789.9 mm^3 versus 456.1 ± 775.2 mm^3 (FBP versus AIDR). Bland-Altman analysis revealed a bias of -5.6 mm^3 (AIDR-FBP, $P = .31$, paired t test) and limits of agreement of -37.6 and 26.6 mm^3 for mean volumes (Fig 3).

890 Hounsfield units [HU]). On the basis of the segmentation of the aneurysm and the attached vessel system, a single surface model was generated by using the marching cube algorithm. To separate the aneurysm structure from the vessels, the observer manually selected a number of points representing the cutting line at the

Pulsatility
Mean pulsatility was 1.095 ± 0.082 mm^3 versus 1.099 ± 0.088 mm^3 (FBP versus AIDR), and Bland-Altman analysis revealed a bias of 0.003 (AIDR-FBP, $P = .62$, paired t test), with limits of agreement between -0.03 and 0.04 (Fig 4).

DISCUSSION

Analysis of the pulsations of cerebral aneurysms could improve the understanding of mechanisms involved in their enlargement and rupture and increase the accuracy of risk prediction of unruptured aneurysms. Previous studies found volume changes of cerebral aneurysms within the cardiac cycle of approximately 5%.[1] These pulsations did not differ significantly from those of normal cerebral arteries but showed a tendency toward larger values. Due to the small excursions of the aneurysm wall, pulsation analysis is technically challenging and improving its accuracy is demanding. IR methods have been shown to improve measurement precision of vessel diameter in a phantom study, a finding from which aneurysm pulsation analysis could benefit. We compared pulsations of 10 cerebral aneurysms from FBP and AIDR reconstructed datasets to analyze the effect size in vivo. No significant changes were observed in absolute aneurysm volumes and pulsations between images reconstructed with IR and AIDR. However, vessel sharpness, one of AIDR's characteristics for improving measurement accuracy, was increased, a finding that just missed statistical significance.

The aforementioned phantom study investigated the influence of wall thickness, intraluminal attenuation, and the reconstruction method on diameter measurement. In our study, the wall thicknesses of aneurysms were essentially unknown but could be estimated by the results of previous reports. In a pathologically based study, the wall thickness was found to be 0.25 mm for 10-mm[13] aneurysms, and an MR imaging–based study found a wall size of 0.6 mm.[14] Mean intra-aneurysmal attenuation was 430 HU, ranging from 223 to 555 HU for the aneurysms, due to the capture of the bolus in first-pass 4D-CTA. Of the 9 groups in the phantom study, for the one comparable to our samples with respect to wall thickness (0.5 mm) and intraluminal attenuation (396 HU), a difference in diameter measurement between FBP and IR images could not be proved. While vessel diameters were overestimated with both reconstruction methods, IR reduced measurement errors significantly in larger-diameter vessels and with higher intraluminal attenuation. Our findings in humans reflect these results by showing smaller volumes in all aneurysms in the AIDR group. However, this finding did not reach a statistically significant level. For a small effect size as found in our study, a much larger sample size is needed to achieve sufficient statistical power.

The effect of IR on vessel delineation is attributed to its ability to improve resolution, reduce image noise, and enhance edges.[15] The examination of image resolution with respect to the reconstruction method is beyond the scope of this article and has been shown in previous examinations.[16] AIDR-reconstructed images expectedly showed reduced overall noise levels, and intra-aneurysmal noise was decreased by 28% (Fig 4). The ability of IR to reduce noise and enhance edges at the same time distinguishes it from FBP reconstruction, which compromises between these as it uses a filter kernel. A quantitative measure for edge sharpness is the length of the attenuation profile at the vessel border, ranging from 10% to 90% of the maximum intraluminal attenuation. The previously described phantom study also examined the influence of wall thickness, intraluminal attenuation, and reconstruction methods on this edge sharpness. IR images showed shorter edges throughout all groups. Edge lengths in our study just missed a

statistically significant level but showed a tendency toward shorter values in AIDR-reconstructed images as seen in the phantom study (Fig 2). There, vessels with 0.5-mm walls did not show an edge profile corresponding to the actual vessel wall as was seen in the thicker-walled vessels. The lack of depiction of the wall in thin-walled vessels was attributed to reconstruction blur and might be the major source of the lack of improvement of accuracy in measuring vessel diameters in this group. With an estimated wall thickness of 0.25 mm in aneurysms in vivo, this effect is even more pronounced.

Due to the small sample size, our study lacks the statistical power to draw further conclusions. Hence, the absence of a significantly different absolute volume or pulsation fraction does not translate into a lack of improvement of accuracy by IR in pulsation analysis. The effect size is small, necessitating large study groups. However, further effort should be made because our results show the applicability of the findings of a well-controlled in vitro study that proved the superiority of IR methods in the diameter measurement of vessels. Furthermore, IR methods from different vendors may have variable effects on edge enhancement and could show a larger improvement of accuracy for this specific application.

CONCLUSIONS

IR methods do not increase the accuracy of pulsation measurements of cerebral artery aneurysms in vivo. This finding might be mainly due to their small wall size.

REFERENCES

1. Kuroda J, Kinoshita M, Tanaka H, et al. Cardiac cycle-related volume change in unruptured cerebral aneurysms: a detailed volume quantification study using 4-dimensional CT angiography. *Stroke* 2012;43:61–66
2. Umeda Y, Ishida F, Hamada K, et al. Novel dynamic four-dimensional CT angiography revealing 2-type motions of cerebral arteries. *Stroke* 2011;42:815–18
3. Yaghmai V, Rohany M, Shaibani A, et al. Pulsatility imaging of saccular aneurysm model by 64-slice CT with dynamic multiscan technique. *J Vasc Interv Radiol* 2007;18:785–88
4. Matsumoto M, Sasaki T, Suzuki K, et al. Visualizing the dynamics of cerebral aneurysms with four-dimensional computed tomographic angiography. *Neurosurgery* 2006;58:E1003, author reply E1003
5. Kato Y, Hayakawa M, Sano H, et al. Prediction of impending rupture in aneurysms using 4D-CTA: histopathological verification of a real-time minimally invasive tool in unruptured aneurysms. *Minim Invasive Neurosurg* 2004;47:131–35
6. Ishida F, Ogawa H, Simizu T, et al. Visualizing the dynamics of cerebral aneurysms with four-dimensional computed tomographic angiography. *Neurosurgery* 2005;57:460–71, discussion 460–71
7. Hayakawa M, Katada K, Anno H, et al. CT angiography with electrocardiographically gated reconstruction for visualizing pulsation of intracranial aneurysms: identification of aneurysmal protuberance presumably associated with wall thinning. *AJNR Am J Neuroradiol* 2005;26:1366–69

8. Suzuki S, Machida, H, Tanaka I, et al. Vascular diameter measurement in CT angiography: comparison of model-based iterative reconstruction and standard filtered back projection algorithms in vitro. *AJR Am J Roentgenol* 2013;200:652–57

9. Ziegler A, Köhler T, Proksa R. Noise and resolution in images reconstructed with FBP and OSC algorithms for CT. *Med Phys* 2007; 34:585–98

10. Sprawls P. AAPM tutorial: CT image detail and noise. *Radiographics* 1992;12:1041–46

11. Machida H, Takeuchi H, Tanaka I, et al. Improved delineation of arteries in the posterior fossa of the brain by model-based iterative reconstruction in volume-rendered 3D CT angiography. *AJNR Am J Neuroradiol* 2013;34:971–75

12. Machida H, Tanaka I, Fukui R, et al. Improved delineation of the anterior spinal artery with model-based iterative reconstruction in CT angiography: a clinical pilot study. *AJR Am J Roentgenol* 2013; 200:442–46

13. Steiger HJ, Aaslid R, Keller S, et al. Strength, elasticity and viscoelastic properties of cerebral aneurysms. *Heart Vessels* 1989;5:41–46

14. Park JK, Lee CS, Sim KB, et al. Imaging of the walls of saccular cerebral aneurysms with double inversion recovery black-blood sequence. *J Magn Reson Imaging* 2009;30:1179–83

15. Beister M, Kolditz D, Kalender WA. Iterative reconstruction methods in X-ray CT. *Phys Med* 2012;28:94–108

16. Suzuki S, Machida H, Tanaka I, et al. Measurement of vascular wall attenuation: comparison of CT angiography using model-based iterative reconstruction with standard filtered back-projection algorithm CT in vitro. *Eur J Radiol* 2012;81:3348–53

ELSEVIER
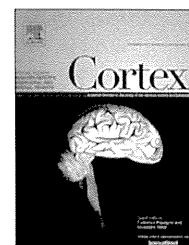
Letter to the editor

Genetic risk variants of schizophrenia associated with left superior temporal gyrus volume

CrossMark

Kazutaka Ohi [a,b], Ryota Hashimoto [a,c,*], Masashi Ikeda [d], Fumio Yamashita [e], Masaki Fukunaga [f], Kiyotaka Nemoto [g], Takashi Ohnishi [h,i], Hidenaga Yamamori [a,j], Yuka Yasuda [a], Michiko Fujimoto [a], Satomi Umeda-Yano [j], Yoshiyuki Watanabe [k], Nakao Iwata [d], Daniel R. Weinberger [l] and Masatoshi Takeda [a,c]

[a] Department of Psychiatry, Osaka University Graduate School of Medicine, Osaka, Japan
[b] National Hospital Organization, Yamato Mental-Medical Center, Nara, Japan
[c] Molecular Research Center for Children's Mental Development, United Graduate School of Child Development, Osaka University, Osaka, Japan
[d] Department of Psychiatry, Fujita Health University School of Medicine, Aichi, Japan
[e] Division of Ultrahigh Field MRI, Institute for Biomedical Sciences, Iwate Medical University, Iwate, Japan
[f] Biofunctional Imaging, Immunology Frontier Research Center, Osaka University, Osaka, Japan
[g] Department of Neuropsychiatry, Institute of Clinical Medicine, University of Tsukuba, Ibaraki, Japan
[h] Department of Psychosomatic Research, National Institute of Mental Health, National Center of Neurology and Psychiatry, Tokyo, Japan
[i] CNS Science Department, Scientific Affairs Division, Janssen Pharmaceutical K.K., Tokyo, Japan
[j] Department of Molecular Neuropsychiatry, Osaka University Graduate School of Medicine, Osaka, Japan
[k] Department of Radiology, Osaka University Graduate School of Medicine, Osaka, Japan
[l] Lieber Institute for Brain Development, Johns Hopkins University Medical Campus, Baltimore, MD, USA

Schizophrenia is a common and complex psychiatric disease with a high estimated heritability of approximately 80% (Sullivan, Kendler, & Neale, 2003), and hundreds of common single-nucleotide polymorphisms (SNPs) are weakly implicated in the pathogenesis of schizophrenia (Purcell et al.,

2009). Gray matter volume (GM) in brain also has an estimated heritability of approximately 60—90% in healthy subjects (Thompson et al., 2001) and reduced GM volumes in patients with schizophrenia have been frequently reported (Chan, Di, McAlonan, & Gong, 2011). A single polygenic

* Corresponding author. Molecular Research Center for Children's Mental Development, United Graduate School of Child Development, Osaka University, D3, 2-2, Yamadaoka, Suita, Osaka, 565-0871, Japan.
E-mail address: hashimor@psy.med.osaka-u.ac.jp (R. Hashimoto).

schizophrenia score (PSS), which was calculated by combining the additive effects of thousands of common independent SNPs weakly associated with schizophrenia explained approximately 3% of the variance in liability for schizophrenia in independent subjects (Purcell et al., 2009). A recent study found that PSS predicts the total brain (TB) and white matter volumes (WM) but not the GM, explaining approximately 5% of the variance in the TB and WM (Terwisscha van Scheltinga et al., 2013). However, it remains unclear whether PSS affects variation in specific GM. Therefore, we investigated the effect of PSS on GM, using (i) voxel-based morphometry (VBM) and (ii) VBM-based region of interest (ROI) methods.

For PSS, the odds ratios for genome-wide SNP data were calculated in a discovery Japanese genome-wide association study (JPN_GWAS) sample including 560 patients with schizophrenia and 548 healthy subjects (Ikeda et al., 2011). On the basis of the genomic-control adjusted p-values in an allele-wise association analysis from the discovery sample, nominally associated alleles at the following liberal significance threshold (P_T) were selected: $P_T \leq .1$, $P_T \leq .2$, $P_T \leq .3$, $P_T \leq .4$, and $P_T \leq .5$. Of 67,315 independent SNPs remained after pruning, the numbers of SNPs at each P_T are as follows; $P_T \leq .1$ ($n = 7,332$), $P_T \leq .2$ ($n = 14,294$), $P_T \leq .3$ ($n = 21,205$), $P_T \leq .4$ ($n = 27,921$), and $P_T \leq .5$ ($n = 34,523$). These data were used to calculate individual PSSs in our target sample of 160 patients with schizophrenia and 378 healthy subjects. The structural images in the target sample were acquired using a 1.5T GE Magnetic Resonance Imaging (MRI) scanner, and the MRI images were processed using the VBM8 toolbox in Statistical

Parametric Mapping 8 (SPM8). Detailed information regarding the subjects and methods is provided in the Supplementary Materials and Methods and Table S1. Written informed consent was obtained from all subjects after the procedures had been fully explained. This study was performed in accordance with the World Medical Association's Declaration of Helsinki and was approved by the Research Ethical Committee of Osaka University.

First, to identify brain regions related to PSS based on each threshold, we conducted a whole-brain search in patients with schizophrenia and healthy subjects using a multiple regression model in SPM8. Age, gender and diagnosis were included as covariates. As we found a marginal interaction between diagnosis and PSS on the left superior temporal gyrus (STG), an area of the brain reported to have reduced GM in high-risk individuals and first-episode and chronic schizophrenia patients (Chan et al., 2011) (a maximum of $T = 4.44$ and $P_{FWE} = .075$ at $P_T \leq .5$) (Fig. S1), we next performed separate whole-brain searches to examine the effects of PSS in patients with schizophrenia and healthy subjects. In the patients, PSS was significantly negatively correlated with the local GM in the left STG at the different P_T-values at the whole-brain corrected level ($P_{FWE} < .05$, a maximum of $T = 5.04$ and $P_{FWE} = .012$ at $P_T \leq .3$) (Fig. 1). Higher PSSs were associated with smaller left STG volumes. The STG was the only region showing the association. Such effects were similarly found at the $P_T \leq .2$ ($T = 4.75$, $P_{FWE} = .037$) to $P_T \leq .5$ ($T = 4.73$, $P_{FWE} = .040$) threshold levels, indicating that many more SNPs based on threshold levels more lenient than $P_T \leq .2$ are predictive of
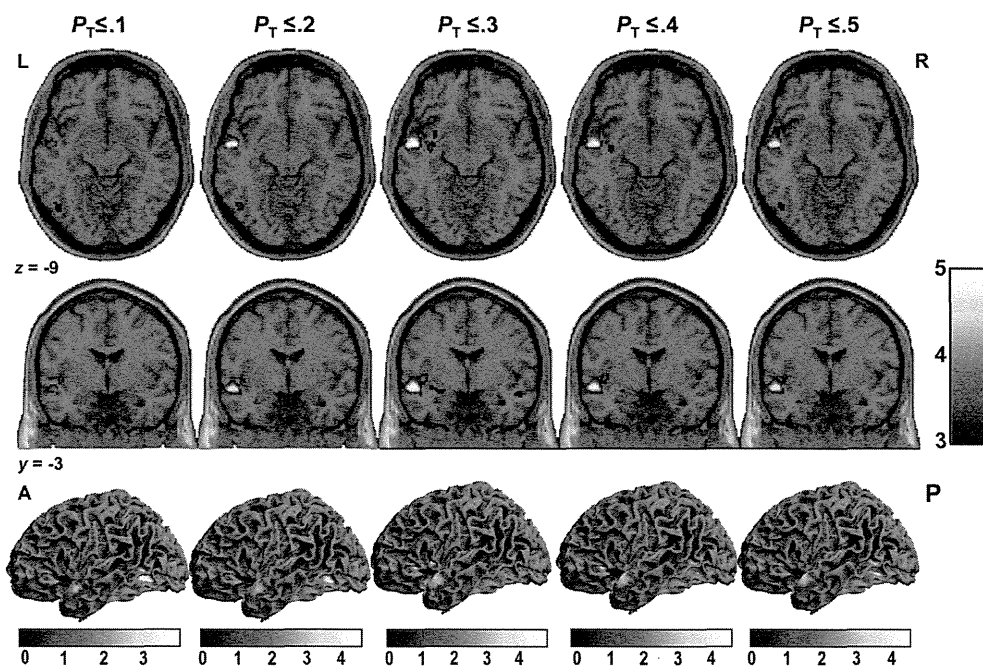
Fig. 1 — Impacts of polygenic scores on gray matter volume in patients with schizophrenia. The effects of PSS based on each threshold ($P_T \leq .1$, $P_T \leq .2$, $P_T \leq .3$, $P_T \leq .4$, and $P_T \leq .5$) on the gray matter volume are shown according to the t values showed by the colored bars. The most significant region of PSS association was in the left superior temporal gyrus (Talairach coordinates of peak voxel: −50, −3, −9). The anatomical localizations are displayed on the axial (upper line) and coronal (middle line) sections of a normal MRI spatially normalized to the Montreal Neurological Institute template. Z and y represent the z and y coordinates in Talairach space. The surface-rendered view (lower line) of the brain region correlating with PSS is shown. L, left; R, right; A, anterior; P, posterior.

reduced STG volumes. When including the number of non-missing SNPs, PANSS scores, duration of illness, or antipsychotic dosage as covariates in the VBM analysis, the effects of PSS on the region remained significant ($P_{FWE} < .05$). In contrast, there was no effect of the score on the GM in healthy subjects ($P_{FWE} > .05$).

The STG is involved in auditory processing, the perception of emotions in facial stimuli, and social cognition (Bigler et al., 2007; Radua et al., 2010). To confirm whether the effect at voxel level on the initial VBM analyses is accepted in the larger structural and functional region, we secondly investigated the effects of PSS on calculated total left STG volumes in patients with schizophrenia and healthy subjects using a multiple linear regression model, with the number of nonmissing SNPs as a covariate using PASW18.0 software. Consistent with the VBM results and expected from them, the ROI analysis revealed that the PSS were significantly negatively correlated with the total left STG volume at all different P_T-values (a maximum $R^2 = .032$, $p = .0090$, at $P_T \leq .2$) in the patients (Fig. S2), whereas there was no effect of the score on the region in the controls ($p > .13$). The PSS explained approximately 3.2% of the variance in the total left STG in the patients with schizophrenia, and the effects of PSS on the region reached a peak at $P_T \leq .3$ in the VBM and $P_T \leq .2$ in the ROI analyses. To examine whether there is a strong association of SNPs with the total left STG, we subsequently conducted a GWAS of the region in the same target samples of patients with schizophrenia. We did not observe any association at a widely used benchmark for genome-wide significance ($p > 5.0 \times 10^{-8}$, Figs. S3–S4 and Table S2).

Although Ikeda et al. (2011) reported that there was a significant correlation of the PSSs between the Japanese and UK samples, there are likely many unique risk variants included in the PSS derived in the Japanese dataset. As the genes comprising the PSS in this study are not identical to those in the MRI study of Terwisscha van Scheltinga et al. (2013), we additionally attempted to replicate the association between PSS and TB and WM (Fig. S5). The PSS were marginally negatively correlated with the TB at the $P_T \leq .5$ ($R^2 = .0035$, $p = .049$) and GM at different P_T-values (a maximum $R^2 = .0073$, $p = .015$, at $P_T \leq .5$), whereas there was no effect of the score on the WM ($p > .05$). The reason why we failed to replicate the associations may be caused by false-negative results due to a small number of discovery samples and/or difference of ethnicities between present and previous studies. We used liberal thresholds ($P_T = .1$ to .5) to obtain PSS according to prior studies (Ikeda et al., 2011; Purcell et al., 2009). However, it was more liberal compared to previous study of Terwisscha van Scheltinga et al. (2013) ($P_T = .002$ to .4). The thresholds we used were so liberal as to likely include a large number of false positives.

Substantially larger controls participated in this study. However, there was a lack of the association in the group. As demographic variables in our samples did not match between healthy subjects and patients with schizophrenia, we matched controls to patients for age and sex and additionally performed the VBM analysis, by removing healthy subjects from the total samples. However, the lack of association in the control group did not change. We considered two reasons for the lack of association; 1) The PSS may be related to a genetic

architecture of patients with schizophrenia but not controls because the PSS were scores derived from risk of schizophrenia. 2) The association that we detected in patients may result from a false-positive finding due to small samples.

Our findings suggest that a set of SNPs weakly associated with schizophrenia may have an accumulative effect on the brain structure of patients, but not controls. However, our findings should be carefully interpreted because there has not been enough evidence for the heritability of brain structures in unaffected siblings (Birnbaum & Weinberger, 2013). It is interesting to note that the STG is the only brain region showing significant association with the PSS in our schizophrenia dataset, even though structural imaging studies of patients with schizophrenia have identified other brain regions that show volume differences between patients and controls, and that no associations were found in normal subjects, a considerably larger sample. This selective association with the STG and only in the patients was not expected and must be viewed as preliminary pending further replication.

Acknowledgments

Supplementary data

Supplementary data related to this article can be found at http://dx.doi.org/10.1016/j.cortex.2014.05.011.

REFERENCES

Bigler, E. D., Mortensen, S., Neeley, E. S., Ozonoff, S., Krasny, L., Johnson, M., et al. (2007). Superior temporal gyrus, language function, and autism. Developmental Neuropsychology, 31, 217–238.
Birnbaum, R., & Weinberger, D. R. (2013). Functional neuroimaging and schizophrenia: a view towards effective connectivity modeling and polygenic risk. Dialogues in Clinical Neuroscience, 15, 279–289.
Chan, R. C., Di, X., McAlonan, G. M., & Gong, Q. Y. (2011). Brain anatomical abnormalities in high-risk individuals, first-episode, and chronic schizophrenia: an activation likelihood estimation meta-analysis of illness progression. Schizophrenia Bulletin, 37, 177–188.

Ikeda, M., Aleksic, B., Kinoshita, Y., Okochi, T., Kawashima, K., Kushima, I., et al. (2011). Genome-wide association study of schizophrenia in a Japanese population. *Biological Psychiatry, 69*, 472—478.

Purcell, S. M., Wray, N. R., Stone, J. L., Visscher, P. M., O'Donovan, M. C., Sullivan, P. F., et al. (2009). Common polygenic variation contributes to risk of schizophrenia and bipolar disorder. *Nature, 460*, 748—752.

Radua, J., Phillips, M. L., Russell, T., Lawrence, N., Marshall, N., Kalidindi, S., et al. (2010). Neural response to specific components of fearful faces in healthy and schizophrenic adults. *NeuroImage, 49*, 939—946.

Sullivan, P. F., Kendler, K. S., & Neale, M. C. (2003). Schizophrenia as a complex trait: evidence from a meta-analysis of twin studies. *Archives of General Psychiatry, 60*, 1187—1192.

Terwisscha van Scheltinga, A. F., Bakker, S. C., van Haren, N. E., Derks, E. M., Buizer-Voskamp, J. E., Boos, H. B., et al. (2013). Genetic schizophrenia risk variants jointly modulate total brain and white matter volume. *Biological Psychiatry, 73*, 525—531.

Thompson, P. M., Cannon, T. D., Narr, K. L., van Erp, T., Poutanen, V. P., Huttunen, M., et al. (2001). Genetic influences on brain structure. *Nature Neuroscience, 4*, 1253—1258.

Prevalence and diagnostic performance of computed tomography angiography spot sign for intracerebral hematoma expansion depend on scan timing

Akio Tsukabe · Yoshiyuki Watanabe · Hisashi Tanaka · Yuki Kunitomi · Mitsuo Nishizawa · Atsuko Arisawa · Kazuhisa Yoshiya · Takeshi Shimazu · Noriyuki Tomiyama

Abstract

Introduction The computed tomography angiography (CTA) spot sign correlates with intracerebral hemorrhage (ICH) expansion; however, various diagnostic performances for hematoma expansion, especially in sensitivity, have been reported. We aimed to assess the impact of scan timing of CTA on the diagnostic performance of the CTA spot sign for ICH expansion in two different arterial phases within patients.

Methods Eighty-three consecutive patients with primary ICH who received two sequential CTAs were recruited. Two neuroradiologists reviewed CTAs for CTA spot signs, while one reviewed initial and follow-up non-contrast CT for measuring ICH volume. The time interval between two phases was then calculated, and the diagnostic performance of CTA spot sign in each phase was evaluated.

Results CTA spot signs were observed in 20/83 (24.1 %) patients in the early phase and 44/83 (53.0 %) patients in the late phase. The mean time interval between the two phases was 12.7 s. Sensitivity, specificity, positive predictive value, negative predictive value, and accuracy for hematoma progression of CTA spot sign were 48.1, 87.5, 65.0, 77.8, and 74.7 %, respectively, in early phase and 92.6, 66.1, 56.8, 94.9, and 74.7 %, respectively, in late phase. The CTA spot sign was significantly associated with ICH expansion in early

($P<0.001$) and late ($P<0.00001$) phases (Pearson's chi-square test).

Conclusion A mere 10-s difference in scan timing could make a difference on prevalence and diagnostic performance of the CTA spot sign, suggesting a need for the standardization of the CTA protocol to generalize the approach for effective clinical application.

Introduction

Intracerebral hemorrhage (ICH) has the highest mortality rate and is the most disabling form of all stroke subtypes. About 30–50 % of patients with ICH die within a month of event onset; moreover, about half of these deaths occur within the first 48 h. The most important predictors of outcome after an ICH include ICH volume, Glasgow Coma Scale score, presence of intraventricular blood, and age [1, 2]. Hematoma expansion, another predictor of outcome, usually occurs in the early time of ICH and is strongly associated with poor prognosis [3–6].

The presence of contrast extravasation on computed tomography angiography (CTA) (CTA spot sign) has been associated with increased risk of hematoma expansion and poor outcome in both retrospective and prospective studies [7–16]. Diagnostic performance of CTA spot sign, however, tends to differ widely among previous reports, especially in terms of the sensitivity. Some reports mentioned the importance of scan timing to detect the contrast extravasation; however, it has not been fully analyzed [17]. A prospective large-scale multicentric study "Prediction of hematoma

A. Tsukabe (✉) · Y. Watanabe · H. Tanaka · Y. Kunitomi · M. Nishizawa · A. Arisawa · N. Tomiyama
Department of Diagnostic and Interventional Radiology, Osaka University Graduate School of Medicine, 2-2 Yamadaoka, Suita, Osaka 565-0871, Japan
e-mail: a-tsukabe@radiol.med.osaka-u.ac.jp

K. Yoshiya · T. Shimazu
Department of Traumatology and Acute Critical Medicine, Osaka University Graduate School of Medicine, Suita, Osaka, Japan

growth and outcome in patients with intracerebral hemorrhage using the CT-angiography spot sign (PREDICT)" did not describe the CTA scan time in detail [12]. One study using subanalysis to further investigate this matter revealed that CTA acquisition parameters differ across institutions [13]. Recently, another study indicated the influence of scan phase on prevalence and diagnostic performance of CTA spot sign, by classifying motley CTA data of PREDICT study with HU measurement of arteries and venous sinuses [18]. But, it has yet to be determined how the prevalence and the diagnostic performance of CTA spot sign vary within patients.

Therefore, the purpose of this study was to assess the impact of scan timing on diagnostic performance of CTA spot sign for hematoma expansion from two different arterial phases within patients.

Methods

Study group

We retrospectively reviewed consecutive 188 patients with spontaneous ICH in our stroke unit between January 1, 2009 and June 30, 2014. Patients with underlying aneurysm, vascular malformation, dissection, trauma, ischemic stroke, and tumor were excluded in this list. Of these 188 patients, 131 patients underwent CTA. Of these 131 patients, 20 patients were excluded because they did not undergo CTA within 6 h from symptom onset. Twenty-eight patients were additionally excluded because they got surgical intervention, were discharged or were deceased before follow-up non-contrast CT (NCCT). And, the final study population included 83 patients. Figure 1 shows study selection process. There were 52 men and 31 women. The mean age was 65.7 years (range, 40–96 years). The average time from symptom onset to CT acquisition was 119.6 min with a range of 34 to 335 min.
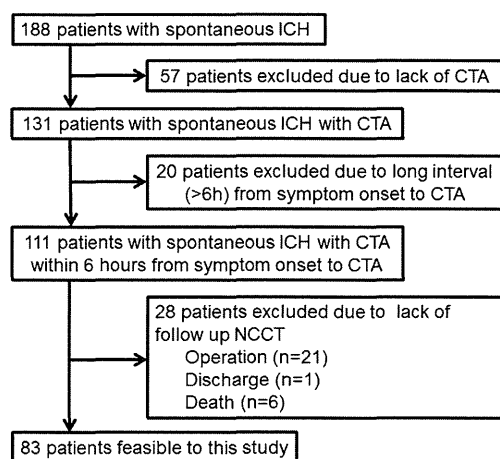
Fig. 1 Flow chart showing study selection process

Thirty-five patients had a hematoma in the putamen, 15 patients had a hematoma in the posterior fossa, 17 patients had a hematoma in the subcortical area, and another 16 had hematomas in the region of the thalamus. For each patient, the following baseline data were collected: age; sex; medical history of hypertension, hyperlipidemia, or diabetes mellitus; antiplatelet use; anticoagulant use; platelet count; international normalized ratio; activated partial thromboplastin time; Glasgow Coma Scale score; systolic blood pressure; body weight at the time of admission; and time from onset to CTA. The study protocol was approved by the local Institutional Review Board of our hospital, and written informed consent from all patients was waived.

Image acquisition

CT examinations were performed with a 64-detector CT scanner from January 1, 2009 to March 31, 2010 with Aquilion64 (Toshiba Medical Systems, Nasu, Japan) and from April 1, 2010 to June 30, 2014 with Definition Flash (Siemens healthcare, Enlargenn, Germany). Precontrast head imaging was followed by two sequential CTAs in all patients. A CTA of the early arterial phase was acquired using the manual bolus tracking technique at the level of the neck. One-hundred milliliters of iohexol (300 mgI/ml) was injected at a rate of 4 cm^3/s from C1 to the vertex or from the aortic arch to the vertex with a 3-s delay. A CTA of the late arterial phase was then acquired sequentially from C1 to the vertex or from the aortic arch to the vertex. The interval of the two CTA scans depended on the machine used and the acquisition range; the minimum interval was 6 s. The acquisition parameters of the NCCT and CTA are shown in Table 1.

Image analysis/interpretation

Two neuroradiologists (with 17 and 5 years of experience in neuroradiology, respectively) blinded to the clinical and radiological outcome of each case reviewed the two arterial phase CTA scans for CTA spot signs, respectively. One of the neuroradiologists was also responsible for assessing initial and follow-up NCCTs for hematoma volume using the ABC/2 method [19]. We measured the hematoma volume of follow-up NCCTs obtained 24 h after initial NCCT. In case surgical intervention was required before 24 h, we used the last follow-up NCCT before surgical intervention. The time interval between early and late arterial phases was obtained at the same level of scan from DICOM data. When assessments from the two neuroradiologists differed, consensus was eventually obtained through discussion. Consistent with previous reports, the presence of a CTA spot sign was defined as one or more 1- to 2-mm foci of enhancement within the hematoma on CTA source images [8]. We defined hematoma expansion as an increase in hematoma volume of >30 % or >6 ml. All

Table 1 Acquisition parameters of CT scans

	Duration	From January 1, 2009 to March 31, 2010	From April 1, 2010 to June 30, 2014
	CT Model	Aquilion64	SOMATOM Definition Flash
NCCT	Acquisition mode	Axial	Axial
	Reconstruction slice thickness (mm)	6&3[a]	6&3[a]
	Field of view (mm)	240	240
	Exposure time (s)	1	1
	Tube voltage (kV)	120	120
	Tube current (ma)	280	470
CTA	Acquisition mode	Helical	Helical
	Reconstruction slice thickness (mm)	0.5	0.6
	Pitch	0.64	0.55
	Field of view (mm)	240	240
	Rotation time (s)	0.5	0.28
	Tube voltage (kV)	120	120
	Tube current (ma)	CT-AEC	CT-AEC

CT-AEC CT auto exposure control, *NCCT* non contrast CT, *CTA* CT angiography

[a] Acquisition parameters for posterior fossa

images were viewed on a PACS (Centricity RA1000, GE HealthCare, Barrington, IL, USA).

Statistical methods

Patients were divided into three groups based on the presence or absence of CTA spot signs during each phase: group 1, no enhancement; group 2, CTA spot sign absent during the early arterial phase and present during the late arterial phase; and group 3, patients with CTA spot sign at both early and late arterial phases. Using either the Mann–Whitney test or Pearson's chi-square test, baseline data and time intervals between the two arterial phases were compared across patient groups. Additionally, the concordance rate of a CTA spot sign between the two neuroradiologists was assessed using kappa analysis. Diagnostic performance of the CTA spot sign was then calculated for each arterial phase according to the following parameters: sensitivity, specificity, positive predictive value (PPV), negative predictive value (NPV), and accuracy. The sensitivity and specificity were compared between CTA spot sign of two arterial phases using McNemar's test. The association of a CTA spot sign in the two arterial phases with hematoma expansion was then analyzed using Pearson's chi-square test. All data analyses were conducted using Stat Flex version 6.0 software (Artech Inc., Osaka, Japan), and we considered P values <0.05 as significant.

Results

Out of the 83 patients, 56 patients did not exhibit changes in hematoma size (67.5 %), while 27 patients were found to have an increase in hematoma size (32.5 %). Time interval between the two arterial phases is shown in Fig. 2, with the mean being 12.7 s (range 6 to 23 s).

Fig. 2 Scan time interval between two arterial phases. The patient numbers of each scan time interval are plotted
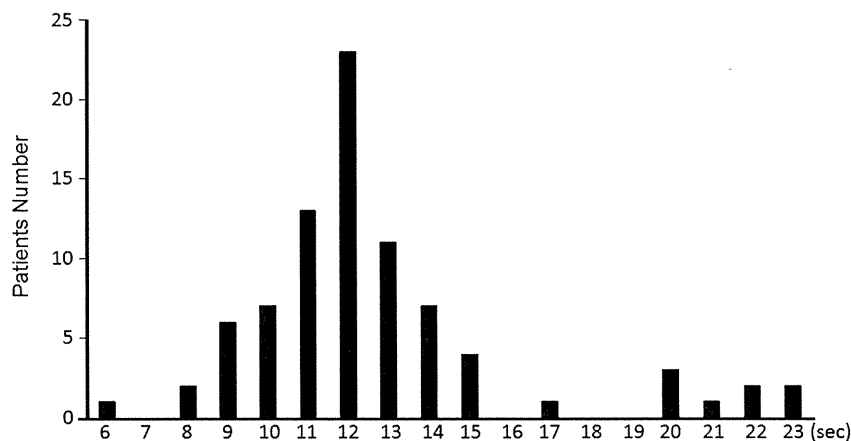
Table 2 Patient characteristics by group

	Group 1 No enhancement (N=39)	Group 2 CTA spot sign(+) In late arterial phase (N=44)	Group 3 CTA spot sign(+) In both arterial phase (N=20)
Demographics			
Age (years)	65.0 (40–92)*	66.2 (43–96)	73.1 (45–96)*
Male gender	21/39 (53.8)	31/44 (70.5)	12/20 (60.0)
Clinical			
GCS score	11.6 (3–15)	10.4 (3–15)	10.7 (3–15)
sBP (mmHG)	200.2 (110–281)	182.7 (103–271)	185.6 (115–239)
BW (kg)	60.8 (37.4–84)	61.0 (33.8–101.1)	58.8 (33.8–101.1)
Hyperlipidemia	7/39 (17.9)	8/44 (18.2)	4/20 (20.0)
Hypertension	31/39 (79.5)	32/44 (72.7)	16/20 (80.0)
Diabetes mellitus	2/39 (5.1)	7/44 (15.9)	4/20 (20.0)
Antiplatelet use	3/39 (7.7)	6/44 (13.6)	4/20 (20.0)
Anticoagulant use	1/39 (2.6)	3/44 (6.8)	2/20 (10.0)
Time from onset to CTA (min)	121.2 (34–335)	118.3 (39–328)	131.3 (49–313)
Time interval between two phases (s)	12.4 (6–23)	13.0 (8–23)	12.7 (9–22)
Process measures			
INR	1.04 (0.86–1.96)	1.30 (0.86–8.76)	1.22 (0.92–2.74)
Platelets (×10⁸ cells/l)	22.1 (12.5–36.3)**,***	20.0 (0.4–110.6)**	21.1 (5.6–110.6)***
APTT (s)	26.7 (17–37)	29.6 (20–77)	30.7 (20–53)

All values are n/N (%) or means (range)

GCS Glasgow Coma Scale, *sBP* systolic blood pressure, *BW* body weight, *INR* international normalized ratio, *APTT* activated partial thromboplatin time, *CTA* CT angiography

*, **, and *** indicate that a significant difference was seen among patient groups with the same mark (Mann–Whitney test)

A CTA spot sign was seen in 20 patients (24.1 %) during the early arterial phase and in 44 patients (53.0 %) during the late arterial phase. Importantly, all patients that exhibited a CTA spot sign during the early arterial phase were positive for a CTA spot sign during the late arterial phase.

Patient clinical characteristics at baseline are summarized in Table 2. The platelet cell counts were significantly different between patient group 1 and patient group 2, and between patient group 1 and patient group 3. The age was significantly different between patient group 1 and patient group 3. No other significant difference was seen in any of the patient baseline data.

Concordance rates for a CTA spot sign in the early and late arterial phase between the two neuroradiologists were 0.97 and 0.90, respectively.

Diagnostic performance of the CTA spot sign for hematoma expansion in each arterial phase is summarized in Table 3. There is a significant difference in sensitivity and specificity between CTA spot sign of two arterial phases (both $P<0.001$). CTA spot sign in the late arterial phase showed much better sensitivity and NPV; however, it showed slightly worse specificity and PPV than in the early arterial phase. Nevertheless, accuracy was the same between phases. Figure 3 shows a representative case where CTA spot sign status is different in each arterial phase.

CTA spot sign was significantly associated with hematoma expansion in both the early arterial phase ($P=0.00037$) and in the late arterial phase ($P<0.000001$) (Pearson's chi-square test).

Table 3 Diagnostic performance of the CTA spot sign in each arterial phase for intracranial hematoma expansion

	Sensitivity	Specificity	PPV	NPV	Accuracy
CTA spot sign of early arterial phase	48.1 %	87.5 %	65.0 %	77.8 %	74.7 %
CTA spot sign of late arterial phase	92.6 %	66.1 %	56.8 %	94.9 %	74.7 %

CTA CT angiography, *PPV* positive predictive value, *NPV* negative predictive value
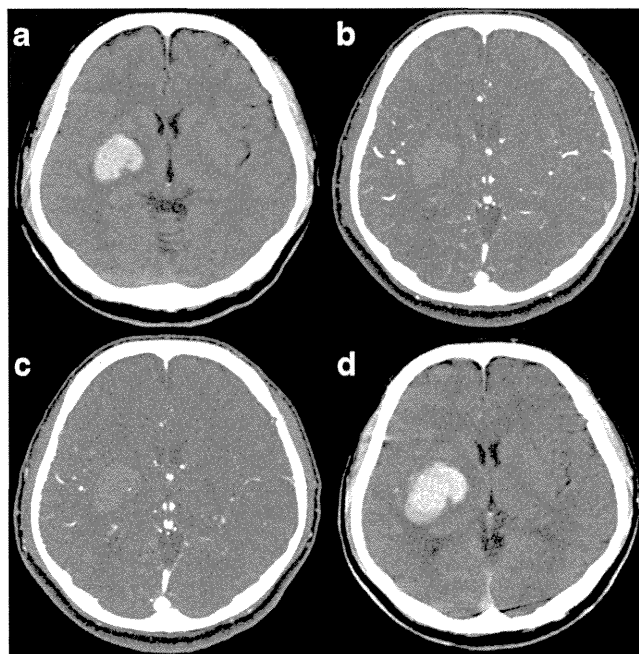
Fig. 3 CT scans of a 59-year-old man that presented with left hemiplegia **a** NCCT shows a putamen hemorrhage. **b** Early arterial phase of CTA does not show punctate foci of intrahematomal contrast. **c** Late arterial phase of CTA shows punctate foci of intrahematomal contrast. **d** NCCT 4 h later shows ICH enlargement

Discussion

Our results showed that the prevalence of a CTA spot sign was heavily influenced by the difference in scan timing with a more than doubled spot sign rate when the scan was delayed by a mere 10 s. The sensitivity and NPV of CTA spot sign in late arterial phase for hematoma expansion were better than those in early arterial phase. The specificity and PPV of CTA spot sign in late arterial phase for hematoma expansion were worse than those in early arterial phase. However, the decrease of specificity was relatively smaller than the increase of sensitivity. The accuracy was the same between the two arterial phases.

Our current study showed relatively low sensitivity in scans acquired during the early arterial phase, while scans taken in the late arterial phase were highly sensitive. Previous reports showed a wide variety of sensitivity. For example, Wada et al. [8] reported a sensitivity of 0.91, while Hallevi et al. [11] reported it as 0.73. Furthermore, the PREDICT study showed relatively low sensitivity at 0.51 [12]. Compared to sensitivity, variation of specificity among previous reports is relatively small. Hallevi et al. [11] reported high specificity (100 %) of a CTA spot sign for predicting hematoma growth. In our study, specificity in the late arterial phase tended to decline; however, it remained relatively high as with previous reports. As previously mentioned, these early reports did not detail their scan timing, even in the PREDICT study. Some institutes used an auto bolus tracking technique, some

used a manual bolus tracking approach, and the others did not use bolus tracking [13]. Recently, Rodoriguez-Luna et al. [18] classified motley CTA data of the PREDICT study into five phases with HU measurement of arteries and venous sinuses and showed that CTA spot sign was depicted more frequently in venous phase and that diagnostic performance of CTA spot sign differed between arterial and venous phases. They reported that sensitivity and specificity of CTA spot sign in arterial phase were 44.6 and 84.2 %, respectively, and that those in venous phase were 73.3 and 72.2 %, respectively. The difference in sensitivity between the arterial and venous phases was bigger than that of specificity. This tendency of their report was similar to our results and consistent with previous literatures. Our results confirm that one of the main reasons of the variance in sensitivity seen throughout the literature is due to differences in scan timing.

Recently, the utility of CT perfusion spot sign was suggested to be more sensitive than CTA spot sign [20, 21], with Sheng-Jun et al. reporting sensitivity at 89.3 % and Koculym et al. reporting sensitivity at 78 %. However, it should be noted that the sensitivity of the CTA spot sign in the late arterial phase (92.6 %) in our study was nearly perfect and superior to these results. Moreover, the dynamism of the CTA spot sign has been demonstrated using a restricted volume CT scanner (Toshiba Aquilion ONE^{TM}) to image the entire brain in a single gantry rotation [22]. From their data, once a CTA spot sign had appeared, it did not disappear; furthermore, the average time to spot appearance was reported to be about 20.8 s, and the maximum density of a spot sign was revealed about 10 s later than spot appearance. This previous study supports our results in that CTA spot sign could be detected in the late arterial phase within all patients that revealed CTA spot signs in the early arterial phase.

Nowadays, aggressive treatments, such as recombinant activated factor VII and intensive blood pressure reduction are suggested to provide a good prognosis for patients with ICH [23–25]. CTA spot sign is expected as one of the selection tools to identify the patients with hematoma expansion and clinical deterioration; therefore, technical standardization is essential for clinical use of this selection tool, especially for multi-center studies. From our data, the accuracy of CTA spot sign did not differ across the phases of CTA within patients. It is preferable to decide the scan timing of CTA with choosing whether high sensitivity or high specificity. When high specificity is required, we should obtain CTA in the early arterial phase. However, determining the optimal timing for obtaining CTA in the early arterial phase is very challenging because physiological variables like blood pressure, arterial resistance, cardiac output, and heart rate will be different among patients. Therefore, we recommend obtaining the CTA in the late arterial phase, around 50 s after contrast material injection as a patient selection tool for advanced treatment with focus on high sensitivity.

This study had some limitations. This was a retrospective, single-center study that contained a relatively small number of patients. Additionally, because there were only a few records concerning scan timing of the early arterial phase from the beginning of the contrast material injection, we only discussed the difference between the two arterial phases. However, it was important that a small difference in scan timing (~10 s) made a big difference in prevalence and diagnostic performances in this study. Therefore, we think the timing of the first arterial phase was not so important for this study. Lastly, some cases had relatively large differences in the time interval of CTAs (~20 s).

Conclusions

We found that small differences in scan timing made a significant impact on prevalence and diagnostic performance of the CTA spot sign within patients. This finding helps explain some of the variations in diagnostic performance in previous reports. Standardization of the CTA protocol is needed to effectively employ this patient selection tool for advanced treatment.

Ethical standards and patient consent We declare that all human and animal studies have been approved by the our hospital's Institutional Review Board and have therefore been performed in accordance with the ethical standards laid down in the 1964 Declaration of Helsinki and its later amendments. We declare that patient consent was waived due to the retrospective nature of this study.

Conflict of interest We declare that we have no conflict of interest.

References

1. Qureshi AI, Mendelow AD, Hanley DF (2009) Intracerebral haemorrhage. Lancet 373(9675):1632–1644. doi:10.1016/s0140-6736(09)60371-8
2. van Asch CJ, Luitse MJ, Rinkel GJ, van der Tweel I, Algra A, Klijn CJ (2010) Incidence, case fatality, and functional outcome of intracerebral haemorrhage over time, according to age, sex, and ethnic origin: a systematic review and meta-analysis. Lancet Neurol 9(2):167–176. doi:10.1016/s1474-4422(09)70340-0
3. Broderick JP, Brott TG, Duldner JE, Tomsick T, Huster G (1993) Volume of intracerebral hemorrhage. A powerful and easy-to-use predictor of 30-day mortality. Stroke 24(7):987–993
4. Brott T, Broderick J, Kothari R, Barsan W, Tomsick T, Sauerbeck L, Spilker J, Duldner J, Khoury J (1997) Early hemorrhage growth in patients with intracerebral hemorrhage. Stroke 28(1):1–5
5. Davis SM, Broderick J, Hennerici M, Brun NC, Diringer MN, Mayer SA, Begtrup K, Steiner T (2006) Hematoma growth is a determinant of mortality and poor outcome after intracerebral hemorrhage. Neurology 66(8):1175–1181. doi:10.1212/01.wnl.0000208408.98482.99
6. Rodriguez-Luna D, Rubiera M, Ribo M, Coscojuela P, Pineiro S, Pagola J, Hernandez-Guillamon M, Ibarra B, Romero F, Alvarez-Sabin J, Montaner J, Molina CA (2011) Ultraearly

7. hematoma growth predicts poor outcome after acute intracerebral hemorrhage. Neurology 77(17):1599–1604. doi:10.1212/WNL.0b013e3182343387
7. Brouwers HB, Goldstein JN, Romero JM, Rosand J (2012) Clinical applications of the computed tomography angiography spot sign in acute intracerebral hemorrhage: a review. Stroke 43(12):3427–3432. doi:10.1161/STROKEAHA.112.664003
8. Wada R, Aviv RI, Fox AJ, Sahlas DJ, Gladstone DJ, Tomlinson G, Symons SP (2007) CT angiography "spot sign" predicts hematoma expansion in acute intracerebral hemorrhage. Stroke 38(4):1257–1262. doi:10.1161/01.STR.0000259633.59404.f3
9. Ederies A, Demchuk A, Chia T, Gladstone DJ, Dowlatshahi D, Bendavit G, Wong K, Symons SP, Aviv RI (2009) Postcontrast CT extravasation is associated with hematoma expansion in CTA spot negative patients. Stroke 40(5):1672–1676. doi:10.1161/strokeaha.108.541201
10. Delgado Almandoz JE, Yoo AJ, Stone MJ, Schaefer PW, Goldstein JN, Rosand J, Oleinik A, Lev MH, Gonzalez RG, Romero JM (2009) Systematic characterization of the computed tomography angiography spot sign in primary intracerebral hemorrhage identifies patients at highest risk for hematoma expansion: the spot sign score. Stroke 40(9):2994–3000. doi:10.1161/STROKEAHA.109.554667
11. Hallevi H, Abraham AT, Barreto AD, Grotta JC, Savitz SI (2010) The spot sign in intracerebral hemorrhage: the importance of looking for contrast extravasation. Cerebrovasc Dis 29(3):217–220. doi:10.1159/000267842
12. Demchuk AM, Dowlatshahi D, Rodriguez-Luna D, Molina CA, Blas YS, Dzialowski I, Kobayashi A, Boulanger JM, Lum C, Gubitz G, Padma V, Roy J, Kase CS, Kosior J, Bhatia R, Tymchuk S, Subramaniam S, Gladstone DJ, Hill MD, Aviv RI (2012) Prediction of haematoma growth and outcome in patients with intracerebral haemorrhage using the CT-angiography spot sign (PREDICT): a prospective observational study. Lancet Neurol 11(4):307–314. doi:10.1016/s1474-4422(12)70038-8
13. Huynh TJ, Demchuk AM, Dowlatshahi D, Gladstone DJ, Krischek O, Kiss A, Hill MD, Molina CA, Rodriguez-Luna D, Dzialowski I, Silva Y, Czlonkowska A, Lum C, Boulanger JM, Gubitz G, Bhatia R, Padma V, Roy J, Kase CS, Aviv RI (2013) Spot sign number is the most important spot sign characteristic for predicting hematoma expansion using first-pass computed tomography angiography: analysis from the PREDICT study. Stroke 44(4):972–977. doi:10.1161/strokeaha.111.000410
14. Kim J, Smith A, Hemphill JC 3rd, Smith WS, Lu Y, Dillon WP, Wintermark M (2008) Contrast extravasation on CT predicts mortality in primary intracerebral hemorrhage. AJNR Am J Neuroradiol 29(3):520–525. doi:10.3174/ajnr.A0859
15. Thompson AL, Kosior JC, Gladstone DJ, Hopyan JJ, Symons SP, Romero F, Dzialowski I, Roy J, Demchuk AM, Aviv RI (2009) Defining the CT angiography 'spot sign' in primary intracerebral hemorrhage. Can J Neurol Sci 36(4):456–461
16. Wang YH, Fan JY, Luo GD, Lin T, Xie DX, Ji FY, Zhang XT (2011) Hematoma volume affects the accuracy of computed tomographic angiography 'spot sign' in predicting hematoma expansion after acute intracerebral hemorrhage. Eur Neurol 65(3):150–155. doi:10.1159/000324153
17. Becker K, Tirschwell D (2009) Stroke. 'Spotting' patients at the highest risk of hematoma growth. Nat Rev Neurol 5(10):526–528. doi:10.1038/nrneurol.2009.152
18. Rodriguez-Luna D, Dowlatshahi D, Aviv RI, Molina CA, Silva Y, Dzialowski I, Lum C, Czlonkowska A, Boulanger JM, Kase CS, Gubitz G, Bhatia R, Padma V, Roy J, Stewart T, Huynh TJ, Hill MD, Demchuk AM (2014) Venous phase of computed tomography angiography increases spot sign detection, but intracerebral hemorrhage expansion is greater in spot signs detected in arterial phase. Stroke 45(3):734–739. doi:10.1161/strokeaha.113.003007

19. Kothari RU, Brott T, Broderick JP, Barsan WG, Sauerbeck LR, Zuccarello M, Khoury J (1996) The ABCs of measuring intracerebral hemorrhage volumes. Stroke 27(8):1304–1305

20. Koculym A, Huynh TJ, Jakubovic R, Zhang L, Aviv RI (2013) CT perfusion spot sign improves sensitivity for prediction of outcome compared with CTA and postcontrast CT. AJNR Am J Neuroradiol 34 (5):965–970, S961. doi:10.3174/ajnr.A3338

21. Sun SJ, Gao PY, Sui BB, Hou XY, Lin Y, Xue J, Zhai RY (2013) "Dynamic spot sign" on CT perfusion source images predicts haematoma expansion in acute intracerebral haemorrhage. Eur Radiol 23(7):1846–1854. doi:10.1007/s00330-013-2803-4

22. Chakraborty S, Alhazzaa M, Wasserman JK, Sun YY, Stotts G, Hogan MJ, Demchuk A, Aviv RI, Dowlatshahi D (2014) Dynamic characterization of the CT angiographic 'spot sign'. PLoS One 9(3): e90431. doi:10.1371/journal.pone.0090431

23. Mayer SA (2007) Recombinant activated factor VII for acute intracerebral hemorrhage. Stroke 38(2 Suppl):763–767. doi:10.1161/01. str.0000254499.46122.22

24. Anderson CS, Huang Y, Wang JG, Arima H, Neal B, Peng B, Heeley E, Skulina C, Parsons MW, Kim JS, Tao QL, Li YC, Jiang JD, Tai LW, Zhang JL, Xu E, Cheng Y, Heritier S, Morgenstern LB, Chalmers J (2008) Intensive blood pressure reduction in acute cerebral haemorrhage trial (INTERACT): a randomised pilot trial. Lancet Neurol 7(5):391–399. doi:10.1016/s1474-4422(08)70069-3

25. Antihypertensive Treatment of Acute Cerebral Hemorrhage i (2010) Antihypertensive treatment of acute cerebral hemorrhage. Crit Care Med 38(2):637–648. doi:10.1097/CCM.0b013e3181b9e1a5

Movement Disorders

CLINICAL PRACTICE

Official Japanese Version of the International Parkinson and Movement Disorder Society–Unified Parkinson's Disease Rating Scale: Validation Against the Original English Version

Kenichi Kashihara, MD,[1,*] Tomoyoshi Kondo, MD,[2,3] Yoshikuni Mizuno, MD,[4] Seiji Kikuchi, MD,[5] Sadako Kuno, MD,[6] Kazuko Hasegawa, MD,[7] Nobutaka Hattori, MD,[8] Hideki Mochizuki, MD,[9] Hideo Mori, MD,[10] Miho Murata, MD,[11] Masahiro Nomoto, MD,[12] Ryosuke Takahashi, MD,[13] Atsushi Takeda, MD,[14] Yoshio Tsuboi, MD,[15] Yoshikazu Ugawa, MD,[16] Mitsutoshi Yamanmoto, MD,[17] Fusako Yokochi, MD,[18] Fumihito Yoshii, MD,[19] Glenn T. Stebbins, PhD,[20] Barbara C. Tilley, PhD,[21] Sheng Luo, PhD,[21] Lu Wang, MS,[21] Nancy R. LaPelle, PhD,[22] Christopher G. Goetz, MD,[20] MDS-UPDRS Japanese Validation Study Group[a]

Abstract: The International Parkinson and Movement Disorder Society (MDS)-sponsored revision of the Unified Parkinson's Disease Rating Scale (MDS-UPDRS) has been developed and is now available in English. Part of the overall program includes the establishment of official non-English translations of the MDS-UPDRS. We present the process for completing the official Japanese translation of the MDS-UPDRS with clinimetric testing results. In this trial, the MDS-UPDRS was translated into Japanese, underwent cognitive pretesting, and the translation was modified after taking the results into account. The final translation was approved as the Official Working Draft of the MDS-UPDRS Japanese version and tested in 365 native-Japanese–speaking patients with PD. Confirmatory analyses were used to determine whether the factor structure for the English-language MDS-UPDRS could be confirmed in data collected using the Official Working Draft of the Japanese translation. As a secondary analysis, we used exploratory factor analyses to examine the underlying factor structure without the constraint of a prespecified factor organization. Confirmatory factor analysis revealed that Comparative Fit Index for all parts of the MDS-UPDRS exceeded the minimal standard of 0.90, relative to the English version, and therefore the Japanese translation met the prespecified criterion to be designated, called an official MDS translation. Secondary analyses revealed some differences between the English-language MDS-UPDRS and the Japanese translation; however, these differences were considered to be within an acceptable range. The Japanese version of the MDS-UPDRS met the criterion as an Official MDS Translation and is now available for use (www.movementdisorders.org).

The UPDRS has been widely used since the 1980s as a standard clinical rating scale for Parkinson's disease (PD).[1,2] However, increasing evidence indicates that several symptoms frequently experienced by PD patients that affect their quality of life, such as sleep problems, sensory disturbance, urinary problems, constipation, and fatigue, are not adequately evaluated in the original

---

[1]Department of Neurology, Okayama Kyokuto Hospital, Okayama, Japan; [2]Department of Neurology, Wakayama Medical University, Wakayama, Japan; [3]Department of Neurology, Rehabilitation Hananosya Hospital, Tochigi, Japan; [4]Department of Neuroregenerative Medicine, Kitasato University School of Medicine, Kanagawa, Japan; [5]Department of Neurology, National Hospital Organization Hokkaido Medical Center, Hokkaido, Japan; [6]Kyoto Shijo Hospital, Kyoto, Japan; [7]Department of Neurology, National Sagamihara Hospital, Kanagawa, Japan; [8]Department of Neurology, Juntendo University School of Medicine, Tokyo, Japan; [9]Department of Neurology, Osaka University Graduate School of Medicine, Osaka, Japan; [10]Department of Neurology, Juntendo University Koshigaya Hospital, Saitama, Japan; [11]Department of Neurology, National Center of Neurology and Psychiatry Parkinson Disease and Movement Disorder Center, Tokyo, Japan; [12]Department of Neurology and Clinical Pharmacology, Ehime University Graduate School of Medicine, Ehime, Japan; [13]Department of Neurology, Kyoto University Graduate School of Medicine, Kyoto, Japan; [14]Department of Neurology, National Hospital Organization Nishitaga Hospital, Miyagi, Japan; [15]Department of Neurology, Fukuoka University Medical School, Fukuoka, Japan; [16]Department of Neurology, Fukushima Medical University, Fukushima, Japan; [17]Takamatsu Neurology Clinic, Takamatsu, Japan; [18]Department of Neurology, Tokyo Metropolitan Neurological Hospital, Tokyo, Japan; [19]Department of Neurology, Tokai University School of Medicine, Kanagawa, Japan; [20]Department of Neurological Sciences, Rush University Medical Center, Chicago, Illinois, USA; [21]Division of Biostatistics, School of Public Health, University of Texas Health Science Center at Houston, Houston, Texas, USA; [22]Division of Preventive and Behavioral Medicine, University of Massachusetts, Worcester, Massachusetts, USA

UPDRS.[3] In 2001, the International Parkinson and Movement Disorder Society (MDS) sponsored a critique of the UPDRS and subsequently developed a new version of the scale, termed the MDS-sponsored UPDRS revision. This new version, the MDS-UPDRS, was intended to be less ambiguous than its predecessor as well as to incorporate a number of clinically pertinent PD-related problems poorly captured in the original version.[4] In 2008, the MDS-UPDRS successfully passed clinimetric testing with high internal consistency and reliable factor structures for each part of the scale.[4] The new MDS-UPDRS comprises four parts: Part I evaluates nonmotor experiences of daily living, Part II evaluates motor experiences of daily living, Part III evaluates motor function, and Part IV evaluates motor fluctuations and dyskinesia.

After publication of the MDS-UPDRS, the MDS set forth a specific program to designate successful translations of non-English-language versions as official MDS translations. For this purpose, the MDS has set a strict protocol and criteria for testing. Currently, several official translations (Italian,[5] Spanish,[6] French, Estonian, German, and Slovakian) have already been established, and several other language programs are in progress. Herein, we present the scale translation and clinimetric testing results of the Japanese version of the MDS-UPDRS.

Patients and Methods

Translation of the MDS-UPDRS

The MDS-UPDRS was translated into Japanese by a team of natural Japanese speakers fluent in English who belong to the Department of Neurology of Wakayama Medical University in Japan, led by Kondo. The resultant Japanese translation was further reviewed by a team led by Mizuno from the Movement Disorder Society of Japan to establish the original Japanese translation of the MDS-UPDRS. The translation was then back-translated by a team of colleagues fluent in English and Japanese who had not been involved in the original forward translation. The back-translation was reviewed by the administrative team in charge of the overall translation program (Stebbins, Goetz, LaPelle, and Tilley).

Cognitive Pretesting

Cognitive pretesting is a qualitative approach to assess instrument completion in terms of task difficulty for examiner and respondent as well as respondent interest, attention span, discomfort, and comprehension.[7] Where there were observed differences between the back-translated Japanese and English versions, items were selected for cognitive pretesting, along with questions that had been identified during cognitive pretesting of the English version. Cognitive pretesting was performed on the following sections: Part I Hallucinations and Psychosis; Features of Dopamine Dysregulation Syndrome; and Urinary Problems; Part II Freezing; Part III Postural Stability; and Rest Tremor Amplitude; Part IV Time Spent with Dyskinesia; and Functional Impact of Dyskinesia. Three experienced Japanese

movement disorder specialists not involved in the original translation performed cognitive pretesting. Based on the results of the initial cognitive pretesting, additional round(s) of translation, back-translation, and cognitive pretesting could be required. After taking the cognitive pretesting results into account, the final Japanese translation was obtained.

Testing of the Japanese Version of the MDS-UPDRS

A total of 30 experienced Japanese movement disorder specialists were recruited as members of the MDS-UPDRS Japanese version validation team led by Kashihara (members are listed in the Appendix) to examine native-Japanese–speaking PD patients who had provided informed consent. The sample size for the translation study was based on the need for 5 participants per questionnaire item in order to perform the statistical analysis.[8] There are 65 items on the MDS-UPDRS: Thus, a sample of at least 325 was required. Any participants with missing values within a part were excluded from the analysis of that part only. Hence, the sample size could vary by part. The investigators obtained approval to collect the data in accord with relevant institutional ethics policies regarding human subjects. Anonymized patient data were transferred to the analysis team by a secure website. The protocol for validation of the MDS-UPDRS Japanese version was approved by the ethics committees of each institute. Informed consent was obtained from all participants before the study.

Data Analysis

Factor Analysis

M-plus (version 6.11)[9] was used to perform confirmatory and exploratory factor analyses (EFA), because the variables are categorical. We used a weighted least squares with mean- and variance-adjusted weighted least square (WLSMV) approach to factor estimation that minimizes the sum of squared differences between observed and estimated correlation matrices not counting diagonal elements. To assist in interpretation of the factors, we used an orthogonal CF-varimax rotation that constrains the factors to be uncorrelated. These methods were chosen to follow those used in the original examination of the English MDS-UPDRS.[4]

Primary Analysis

We conducted a confirmatory factor analysis (CFA)[10] as the primary analysis of the Japanese data to determine whether the factor structure for the English-language MDS-UPDRS[4] could be confirmed in data collected by using the Japanese translation. This was the primary question of interest. The CFA was conducted separately for the MDS-UPDRS Parts I to IV, with the Japanese data constrained to fall into the factors defined in the English-language data.[4] We evaluated the CFA results based on the comparative fit index (CFI). According to

protocol, to establish a successful translation and earn the designation of "official MDS-UPDRS translation," the CFI for each part (I–IV) of the translated instrument must be 0.90 or greater, relative to the English-language version.[4] Root mean square error of approximation (RMSEA) was also calculated as another test of model fit. RMSEA values <0.05 were considered to be a good fit, and RMSEA values of 0.1 or more were considered to be a poor fit. WLSMV estimators were used to confirm a model fit.

Secondary Analysis

As a secondary analysis, we conducted an exploratory factor analysis[11] for Parts I to IV of the Japanese version of the MDS-UPDRS to explore the underlying factor structure without the constraints of a prespecified factor structure. We used a Scree plot to choose the number of factors to retain for each part. The subjective Scree test[12] is scatter plot of eigenvalues plotted against their ranks with respect to magnitude to extract as many factors as there are eigenvalues that fall before the last large drop (i.e., an "elbow" shape) in the plot. Once the factors were chosen, an item was retained in a factor if the factor loading for the item was 0.40 or greater.

The default estimator for factor analysis in M-plus is unweighted least squares (ULS). When ULS converges, it yields more-accurate parameter estimates and standard errors than does WLSMV. However, WLSMV generally outperforms ULS in convergence rates. Thus, Forero et al.[13] suggest the use of ULS. In the case of nonconvergence, however, they suggest using WLSMV, because this method might converge when ULS does not. In this case, whereas the ULS algorithm did converge, it converged to an incorrect value (i.e., a percent of variance explained that was greater than 1.0), so WLSMV was used.

The chi-square test was used to analyze, additionally, the differences in the distribution of responses for each item of the MDS-UPDRS between PD patients of Japanese and English groups.

Results

Cognitive Pretesting

A total of 12 patients with PD and their examiners were interviewed using a structured interview format typical in cognitive pretesting. During the first round of cognitive pretesting, minor word changes were suggested for features of dopamine dysregulation syndrome, urinary problems, and time spent with dyskinesia. In response to comments from patients and caregivers, we enlarged the size of characters used in questions from Part IB and Part II. No items were identified as problematic during a second round of cognitive pretesting conducted with 10 patients with PD. The modified version of the scale was approved as the Official Working Draft of the Japanese MDS-UPDRS for testing in a larger group of patients with PD.

Data Analysis

Demographics

Participants' demographic characteristics are shown in Table 1. The Japanese data set included 365 native-Japanese–speaking patients with PD who were examined using the MDS-UPDRS. In the Japanese sample, there was a greater proportion of female patients, compared to the English sample. The two cohorts were similar on age and duration of disease, but the distribution of H & Y stages were significantly different between the two cohorts ($P < 0.0005$; Table 1).

Primary Analysis: CFA

Table 2 displays the CFA models for each part of the MDS-UPDRS. For all four parts of the Japanese version, the CFI was 0.93 or greater, in comparison to the English-language factor structure. Our prespecified criterion was a CFI of 0.90 or greater; thus, we conclude that the English factor structure was confirmed in the Japanese data set.

Secondary Analysis: EFA

The factor structure of the EFA for the English version has been used as the basis for all CFAs, but our EFA of the Japanese

TABLE 1 Demographics of Japanese patients with PD in comparison with the MDS-UPDRS (English version) data

	English	Japanese	P Value
Total N	876	365	ns
% male	63.2	45.2	<0.0005
Age (mean ± SD)	68.2 ± 10.8	69.0 ± 9.2	ns
Disease duration (mean years ± SD)	8.3 ± 6.7	7.8 ± 6.1	ns
Years of education	NA	12.6 ± 2.7	ns
H & Y stage			<0.0005
0	0	2	
1	63	28	
2	467	164	
3	174	116	
4	109	42	
5	53	11	

SD, standard deviation; NA, not available; ns, not significant.

TABLE 2 Confirmatory factor analysis model fit

Part I: Nonmotor aspects of experiences of daily living (a two-factor model)[a]
Japanese   CFI = 0.93; RMSEA = 0.09 (351 patients)
English language   CFI = 0.97; RMSEA = 0.05 (849 patients)
Part II: Motor aspects of experiences of daily living (a three-factor model)
Japanese   CFI = 0.99; RMSEA = 0.07 (356 patients)
English language   CFI = 0.99; RMSEA = 0.05 (851 patients)
Part III: Motor examination (a seven-factor model)
Japanese   CFI = 0.94; RMSEA = 0.08 (336 patients)
English language   CFI = 0.95; RMSEA = 0.08 (801 patients)
Part IV: Motor complications (a two-factor model)
Japanese   CFI = 1.00; RMSEA = 0.06 (350 patients)
English language   CFI = 1.00; RMSEA = 0.00 (848 patients)

[a]Dopamine dysregulation syndrome was not included in this analysis because it did not load on any factor in the U.S. version.

data set differs from that of the English-language data set in some aspects. The results of the EFA for the English and Japanese versions are shown in Table 3, including the number of factors and their associated eigenvalues and percent variance.

The Scree plots were used to determine the number of factors to be retained from the EFA. Comparison between the Scree plots for the English and Japanese cohorts revealed similarities in shape of the plots (Fig. 1), but differences were noted in the relationship between factors and their eigenvalues and percent of variance (Table 3): For Part I: Nonmotor aspects of experiences of daily living, we extracted two factors; for Part II: Motor aspects of experiences of daily living, we extracted three components; for Part III: Motor examination, we extracted seven factors; and for Part IV: Motor complications, we extracted two factors.

Chi-square (χ^2) test (Table 4) revealed greater distribution of less-severe scores on the cognitive impairment items (Part I: item 1.1) in the Japanese group, compared to the English group ($\chi^2 = 23.457$; df = 4; $P = 0.0001$). There was no significant difference of the distribution of scores on the hallucinations and psychosis item (Part I: item 1.2) ($\chi^2 = 5.962$; df = 4; not significant). In many other items, PD patients in the English group showed greater distribution of more-severe scores, including depressed mood, pain and other sensations, lightheadedness on standing, fatigue, and sleep problems in Part I; speech, saliva and drooling, doing hobbies and other activities, tremor, and getting out of bed in Part II; speech, facial expression, rigidity, finger tapping, hand movements, pronation supination, toe tapping, leg agility, and tremor in Part III; and time spent with dyskinesia, functional impact of dyskinesias, time spent in the OFF state, complexity of motor fluctuations, and painful OFF-state dystonia in Part IV. Japanese PD patients showed greater distribution in more-severe scores than English groups in items constipation problems in Part I and postural stability in Part III.

Discussion

The overall factor structure of the Japanese version was consistent with the English version based on the CFIs for all four parts of the MDS-UPDRS in the CFA (all CFI ≥0.93). The Japanese scale was confirmed to share a common factor structure with the English scale. Therefore, this version can be designated as the official Japanese version of the MDS-UPDRS.

EFA, in which variability from sample to sample is expected, identified isolated item differences of factor structure between the Japanese and English versions of the MDS-UPDRS. However, the distribution of factors with their associated eigenvalues and percent variances were similar across the two languages.

In our study, female preponderance was noted as the previous study reported from Japan.[14] This may, in part, be because of the longer life expectancy (by approximately 6.5 years) in Japanese women, in comparison to men.

Another interesting difference between the Japanese- and English-language versions data sets for the MDS-UPDRS concerned the pattern of responses to items 1.1 (cognitive impairment) and 1.2 (hallucinations and psychosis). For the

TABLE 3 Comparison of English-language and Japanese exploratory factor structures for parts I to IV of the MDS-UPDRS

Factor	English		Japanese	
	Eigenvalues	Percent Variance	Eigenvalues	Percent Variance
Part I				
1	4.421	34.0	5.045	42.0
2	1.231	9.5	1.244	10.4
3	1.051	8.1	1.081	9.0
4	1.007	7.7	0.866	7.2
5	0.811	6.2	0.721	6.0
6	0.724	5.6	0.642	5.4
7	0.673	5.2	0.594	5.0
8	0.630	4.8	0.508	4.2
9	0.616	4.7	0.472	3.9
10	0.542	4.2	0.375	3.1
11	0.519	4.0	0.288	2.4
12	0.399	3.1	0.160	1.3
13	0.376	2.9		
Part II				
1	6.898	53.1	7.293	56.1
2	1.128	8.7	1.062	8.2
3	1.000	7.7	0.826	6.4
4	0.728	5.6	0.684	5.3
5	0.595	4.6	0.534	4.1
6	0.542	4.2	0.494	3.8
7	0.425	3.3	0.445	3.4
8	0.390	3.0	0.431	3.3
9	0.380	2.9	0.370	2.8
10	0.294	2.3	0.260	2.0
11	0.245	1.9	0.240	1.8
12	0.198	1.5	0.219	1.7
13	0.178	1.4	0.141	1.1
Part III				
1	12.112	36.7	14.451	43.8
2	5.035	15.3	4.190	12.7
3	2.173	6.6	2.429	7.4
4	2.051	6.2	1.961	5.9
5	1.615	4.9	1.668	5.1
6	1.485	4.5	1.238	3.8
7	1.104	3.3	0.922	2.8
8	0.903	2.7	0.793	2.4
9	0.720	2.2	0.685	2.1
10	0.615	1.9	0.596	1.8
11	0.552	1.7	0.558	1.7
12	0.495	1.5	0.514	1.6
13	0.479	1.5	0.472	1.4
14	0.407	1.2	0.360	1.1
15	0.403	1.2	0.348	1.1
16	0.361	1.1	0.330	1.0
17	0.323	1.0	0.246	0.7
18	0.314	1.0	0.233	0.7
19	0.267	0.8	0.203	0.6
20	0.265	0.8	0.194	0.6
21	0.223	0.7	0.183	0.6
22	0.203	0.6	0.147	0.4
23	0.164	0.5	0.138	0.4
24	0.145	0.4	0.115	0.3
25	0.141	0.4	0.099	0.3
26	0.109	0.3	0.058	0.2
27	0.091	0.3	0.027	0.1
28	0.077	0.2	0.013	0.0
29	0.055	0.2	0.004	0.0
Part IV				
1	3.811	63.9	3.656	60.9
2	0.942	15.6	1.210	20.2
3	0.640	10.7	0.725	12.1
4	0.241	4.0	0.168	2.8
5	0.208	3.5	0.130	2.2
6	0.159	2.3	0.111	1.9

Dotted line shows the factors selected in the English cohort.
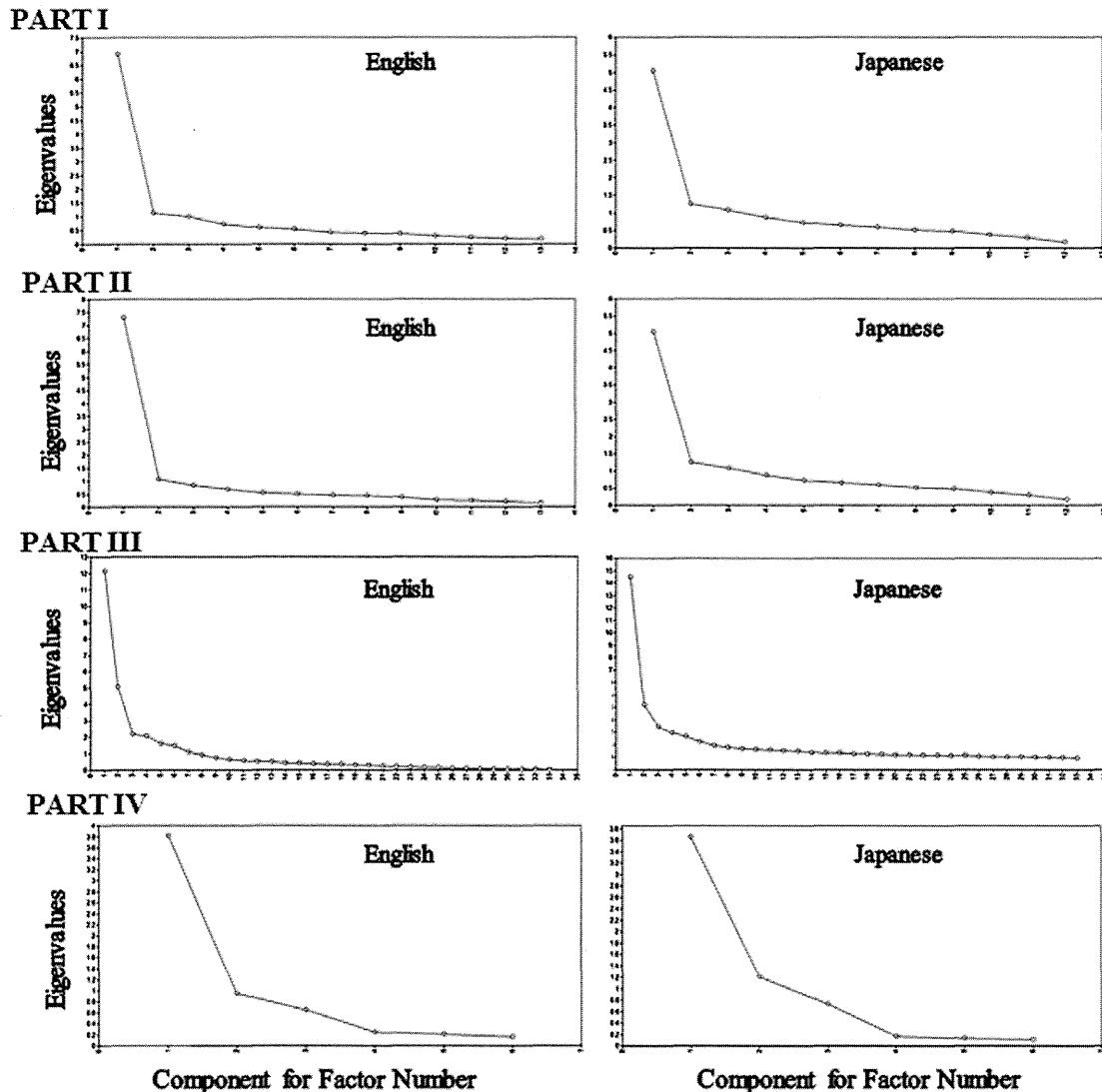
PART I

PART II

PART III

PART IV

Figure 1 Scree plots for the English and Japanese exploratory factor analyses.

hallucination item, the Japanese and English frequencies for each rating option were very similar (77% and 78%, respectively), but cognitive impairment ratings were different in the two cultures. A much greater percentage (62.2%) of Japanese had 0 scores, in comparison to the English-speaking sample (48.9%). In general, among reports in Western cultures, cognitive impairment and hallucinations are shared or overlapping behaviors and such data have been used to argue shared common pathogeneses.[15,16] Results of the chi-square test indicate that severity of motor and nonmotor symptoms are generally more severe in patients of English groups than those of Japanese groups. Even after taking these differences into consideration, the present results from the Japanese sample may indicate that cognitive impairment is less frequent or viewed differently and thereby may be underreported for cultural reasons in Japan, in comparison to the Western culture.

Contrary to majority of items, constipation problems and postural stability were rated more severe in Japanese patients

than English patients. Differences in genetic factor, eating habits, and amount of daily exercise between two populations are possible factors to produce different response to the former item. The reason why postural stability was rated more severely in Japanese groups remains unknown. Factors including examiner's manner to pull patients may be clarified in future.

In conclusion, the CFI for the Japanese version of the MDS-UPDRS was 0.93 or greater. Therefore, the Japanese version meets the criterion for designation as an official translation of the MDS-UPDRS. This is the first Asian- or non-Indo-European-language translation of the MDS-UPDRS. The Japanese version of the MDS-UPDRS is available from the MDS website (http://www.movementdisorders.org/publications/rating_scales/). The establishment of additional non-English translations will further facilitate the understanding of PD symptoms and help accelerate qualified clinical trials and discussions worldwide.

TABLE 4 Distribution of responses by MDS-UPDRS by language[a]

	English		Japanese			English		Japanese	
Part I									
Cognitive impairment*	Frequency	%	Frequency	%	Daytime sleepiness	Frequency	%	Frequency	%
0	428	48.86	227	62.19	0	212	24.2	104	28.49
1	256	29.22	93	25.48	1	216	24.66	73	20.00
2	121	13.81	25	6.85	2	364	41.55	147	40.27
3	53	6.05	17	4.66	3	59	6.74	32	8.77
4	17	1.94	3	0.82	4	16	1.83	8	2.19
999	1	0.11	0	0.00	999	9	1.03	1	0.27
Total	876	100	365	100.00	Total	876	100	365	100.00
Hallucinations and psychosis	Frequency	%	Frequency	%	Pain and other sensations*	Frequency	%	Frequency	%
0	687	78.42	280	76.71	0	303	34.59	148	40.55
1	89	10.16	38	10.41	1	289	32.99	117	32.05
2	51	5.82	26	7.12	2	130	14.84	60	16.44
3	35	4	14	3.84	3	106	12.1	31	8.49
4	13	1.48	4	1.10	4	39	4.45	4	1.10
999	1	0.11	3	0.82	999	9	1.03	5	1.37
Total	876	100	365	100.00	Total	876	100	365	100.00
Depressed mood*	Frequency	%	Frequency	%	Urinary problems	Frequency	%	Frequency	%
0	471	53.77	223	61.10	0	325	37.1	144	39.45
1	265	30.25	84	23.01	1	281	32.08	118	32.33
2	81	9.25	36	9.86	2	137	15.64	60	16.44
3	45	5.14	21	5.75	3	88	10.05	32	8.77
4	12	1.37	0	0.00	4	38	4.34	10	2.74
999	2	0.23	1	0.27	999	7	0.8	1	0.27
Total	876	100	365	100.00	Total	876	100	365	100.00
Anxious mood	Frequency	%	Frequency	%	Constipation problems*	Frequency	%	Frequency	%
0	413	47.15	192	52.60	0	384	43.84	90	24.66
1	307	35.05	116	31.78	1	287	32.76	120	32.88
2	96	10.96	39	10.68	2	119	13.58	74	20.27
3	41	4.68	15	4.11	3	70	7.99	63	17.26
4	17	1.94	1	0.27	4	9	1.03	18	4.93
999	2	0.23	2	0.55	999	7	0.8	0	0.00
Total	876	100	365	100.00	Total	876	100	365	100.00
Apathy	Frequency	%	Frequency	%	Lightheadedness on standing*	Frequency	%	Frequency	%
0	584	66.67	249	68.22	0	490	55.94	238	65.21
1	141	16.1	61	16.71	1	216	24.66	78	21.37
2	88	10.05	27	7.40	2	103	11.76	37	10.14
3	52	5.94	20	5.48	3	51	5.82	10	2.74
4	8	0.91	7	1.92	4	9	1.03	1	0.27
999	3	0.34	1	0.27	999	7	0.8	1	0.27
Total	876	100	365	100.00	Total	876	100	365	100.00
Features of DDS	Frequency	%	Frequency	%	Fatigue*	Frequency	%	Frequency	%
0	747	85.27	315	86.30	0	217	24.77	141	38.63
1	57	6.51	23	6.30	1	335	38.24	128	35.07
2	44	5.02	20	5.48	2	184	21	57	15.62
3	19	2.17	4	1.10	3	81	9.25	33	9.04
4	6	0.68	0	0.00	4	50	5.71	4	1.10
999	3	0.34	3	0.82	999	9	1.03	2	0.55
Total	876	100	365	100.00	Total	876	100	365	100.00
Sleep problems*	Frequency	%	Frequency	%					
0	280	31.96	138	37.81					
1	202	23.06	103	28.22					
2	207	23.63	81	22.19					
3	140	15.98	39	10.68					
4	40	4.57	3	0.82					
999	7	0.8	1	0.27					
Total	876	100	365	100.00					
Part II									
Speech*	Frequency	%	Frequency	%	Doing hobbies and other activities*	Frequency	%	Frequency	%
0	252	28.77	159	43.56	0	227	25.91	130	35.62
1	236	26.94	78	21.37	1	289	32.99	99	27.12
2	233	26.6	82	22.47	2	185	21.12	65	17.81
3	126	14.38	43	11.78	3	81	9.25	41	11.23